Passive Polarization Converter in SiON Technology

Ton Koster and Paul V. Lambeck, *Member, OSA*

***Abstract*—A passive polarization converter has been realized in silicon oxynitride (SiON) technology. The device is a grating assisted codirectional coupler consisting of segments of asymmetrically etched ridge waveguides. By using a double-masking technique, the fabrication of the device is tolerant with respect to the alignment of the required masks. Conversion efficiencies up to 0.98 ($\mathrm{TE} \rightarrow \mathrm{TM}$ and $\mathrm{TM} \rightarrow \mathrm{TE}$) and insertion losses of 3 dB/cm have been measured. Using 2-D beam propagation method simulations, an observed beat pattern in the converter could be explained as due to a leaky mode, which is captured in the grating structure.**

***Index Terms*—Design, grating, polarization conversion, SiON.**

I. Introduction

THE existence of two states of polarization propagating through monomodal integrated optical waveguides poses problems to some integrated optical circuits and is exploited in others. An example of the former is an add drop multiplexer [1], of which the peformance must be polarization independent due to the unknown state of polarization coming out of the input fiber. An example of the latter is a polarimeter [2], which is a sensor based on the different sensitivities of modes of both polarizations to the measurand. If the existence of modes of both polarizations poses a problem to a given integrated optical device, there are two ways to eliminate it. One is the realization of polarization-independent devices [3], thereby posing severe limitation/requirements to both the design and technology. Another is the implementation of polarization manipulating functionalities in the devices, such as a polarization converter [4], which enables transfer of optical power from one state of polarization to the other and vice versa. For many devices exploiting the TE/TM behavior of light, such as the polarimeter, the polarization converter is an essential basic building block.

Both active [3] and passive [4] converters have been reported in literature. Here, active refers to the use of physical cross effects for inducing the grating that is needed for obtaining polarization conversion. Active converters have the advantage that the amount of conversion can be controlled by changing the driving power, while in the optoacoustic case, also the grating period can be adjusted [3]. However, the use of most of the active converters reported up to now [3], [5] is limited by the need for (expensive) materials, which should show physical cross effects (such as electrooptical or acoustooptical) and should have a crystal structure with a symmetry that permits coupling between both types of polarization. In the case of acoustooptical devices, an additional drawback is the use of high-frequency control electronics [3], which limits low-cost commercial application of these devices. Contrary to active converters, in passive converters there are fewer restrictions with respect to the materials used and, in general, a much simpler fabrication technology is possible. If required by the application, wavelength tunability can be added using the thermooptical effect [6], [7] which, as opposed to the electro- and acoustooptical effect, does not require any expensive material or technology.

In 1990, the first paper on a passive polarization converter was published by Shani *et al.* [4]. Since then, various groups have published results about passive polarization converters based mainly on two different principles. One uses waveguides with strongly hybrid modes in order to obtain polarization conversion without using periodic structures. For example, the converters in [8], [9]. The other principle implies the use of asymmetrical grating structures in grating assisted couplers such as reported in [10] and [11]. The converter presented here is based on such a grating structure.

In this paper, we present a passive converter realized in Silicon Oxynitride (SiON)technology. The waveguide system consists of a high-index Si_3N_4 core layer in between two low index SiO_2 layers. In this layer system, the ridge-type channel modes are nearly similar to slab modes, insofar that they show very small nondominant field components. Hence, converters based on strongly hybrid modes cannot be implemented in this material system, and grating type polarization structures have to be used. The converter reported here is the first realization [12] of a converter based on segments of asymmetrical etched ridge waveguides, as proposed by [13]. The structure has been designed in order to minimize the effect of technological uncertainties on the conversion wavelength. Furthermore, by using a double-masking technique, the fabrication can be made very tolerant with respect to the alignment of the converter mask to the waveguide mask. The device shows a narrow-band wavelength response, offering the possibility of implementing it as a wavelength filter in devices such as add-drop multiplexers.

In Section II, the structure and principle of the converter are explained. After a brief discussion of the device fabrication in Section III, experimental results are presented in Section IV. In Section V, the obtained experimental results are compared to results obtained in literature. Also, possible applications of the converter are shortly discussed. In Section VI, a summary is given.

II. Structure and Design

In this section, the device principle will be briefly discussed and the designing process, in which a tolerance analysis of the converter plays a main part, is presented. Due to the specific application, which in our case is an integrated optical sensor of

Manuscript received November 20, 2000. This work was supported by the Technology Foundation (STW), T.E.L. 44.3474.

The authors are with the Lightwave Devices Group, Mesa+ Research Institute, University of Twente, 7500 AE Enschede, The Netherlands.

Publisher Item Identifier S 0733-8724(01)04590-X.

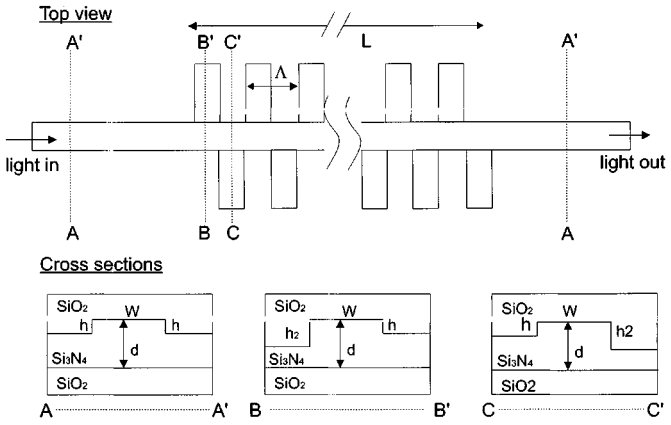

Fig. 1. A top view and cross sections of the polarization converter.

specific type [14], the converter presented here is designed for a wavelength of 655 nm. However, the design methodology, based on an optimization with respect to device reproducibility, can be generally applied for every operation wavelength.

The converter is a codirectional grating assisted coupler consisting of segments of asymmetrical etched ridge waveguides, as shown in Fig. 1. Due to the induced asymmetry, there is a slight tilt of the optical birefringence axis with respect to the symmetrical layer system. As a result, there is a nonzero field overlap between the TE and TM fields in adjacent grating segments. At each transition between adjacent segments, the polarization angle is slightly rotated for the resonance wavelength λ_r given by

$$\lambda_r = \Lambda(N^c_{\mathrm{TE}} - N^c_{\mathrm{TM}}) \equiv \Lambda \Delta N^c_{\mathrm{TE-TM}}. \tag{1}$$

Here, Λ is the grating period and N^c_{TE} and N^c_{TM} are the effective indexes of the TE and TM channel mode, respectively. It should be noted that (1) is exact, as in our case both grating segments are each others' mirror image with respect to the center of the ridge waveguide, so the TE mode in both segments, just as the TM modes, have the same effective index.

The layer stack in which the converter is realized is shown in Fig. 1; it consists of a high index $\mathrm{Si_3N_4}$ core layer in between two $\mathrm{SiO_2}$ layers. This layer stack was chosen because of the intended application circuits in which the converter should be incorporated. However, the presented layer stack also has additional advantages for the converter. First, these layers can be grown/deposited very accurately with respect to their refractive indexes and to the thickness of the $\mathrm{Si_3N_4}$ layer, thereby increasing the reproducibility of the converter. Second, using this high refractive index contrast layer system, a large difference between the effective indexes of the TE and TM mode is obtained, resulting in grating periods of acceptable length.

There are several boundary conditions to the design. First, the converter should be mono modal, allowing only the lowest order TE and TM to propagate through the structure. For the given operation wavelength and layer stack, this limits the core layer thickness to a maximum of 250 nm, as can be calculated by the mono modal condition $V < \pi$, with V the normalized core thickness [15]. Using the effective index method (EIM) and ignoring the asymmetry in a first stage, the monomodal condition in the lateral direction can be expressed as

$$\frac{2}{\lambda}\sqrt{2N^s_i \frac{\partial N^s_i}{\partial d}} W\sqrt{h} < 1 \tag{2}$$

with N^s_i the effective index of the slab modes for TE or TM for a core thickness d, ridge height h, and ridge width W. Second, the coupling to radiation modes must be absent for first-order coupling, which puts a lower limit to the allowed grating period Λ,

$$\Lambda > \frac{\lambda_r}{N^c_{\mathrm{TM}} - n_{\mathrm{SiO_2}}} \tag{3}$$

with $n_{\mathrm{SiO_2}}$ the refractive index of the $\mathrm{SiO_2}$ layer. Third, the converter should be fabrication tolerant regarding its resonance wavelength and the coupling strength, i.e., the design has to take technological uncertainties into account.

Most important is the control of the resonance wavelength λ_r which is a function of the effective index difference between the TE and TM mode. Using the EIM, it can easily be shown that the effective indexes of the TE and TM channel modes, N^c_i lie in the interval

$$N^s_i(d) - \frac{\partial N^s_i(d)}{\partial d} h < N^c_i < N^s_i(d) \tag{4}$$

where i stands for TE or TM; here the higher order terms in the Taylor expansion have been neglected. The superscript s again refers to the slab modes in a core layer with thickness d, and c refers to the channel modes of the ridge waveguide.

As there is a high contrast layer system in the vertical direction, the ridge height h has to be very small (0–2 nm combined with a ridge width W in between 2 and 5 μm) in order to obtain a monomodal system, and, hence, the range in which the effective index difference lies is very narrow. From (4), it can be noted that if $\partial \Delta N^s_{\mathrm{TE-TM}}(d)/\partial d = 0$, $\Delta N^c_{\mathrm{TE-TM}}$ should be independent of h within the validity of our approximations.

Now, we will investigate the influence of h_2 on $\Delta N_{\mathrm{TE}} - \mathrm{TM}^c$. In the EIM, the asymmetry manifests itself in the normalized a-parameter of the equivalent slab guides in the lateral direction. Because of the small lateral effective index contrast, this a-parameter is in good approximation identical for the TE and TM slab guides,

$$\begin{aligned} a =& \frac{(N^s_{d-h})^2 - (N^s_{d-h_2})^2}{(N^s_d)^2 - (N^s_{d-h})^2} \\ \approx& \frac{2N^s(d)\frac{\partial N^s}{\partial d}(h_2 - h)}{2N^s(d)\frac{\partial N^s}{\partial d}h} \\ =& \frac{h_2 - h}{h}. \end{aligned} \tag{5}$$

The influence of h_2 on $\Delta N^c_{\mathrm{TE-TM}}$ is generally much smaller than the influence of h on $\Delta N^c_{\mathrm{TE-TM}}$, especially in the case of a large asymmetry parameter (> 10) which, as will be seen later on, is the case with the presented converter.

Regarding all geometrical parameters, it can be concluded that the effective index difference, and, hence, the resonance wavelength, is mainly dependent on the core layer thickness.

TABLE I
TECHNOLOGICAL PARAMETERS AND THE TECHNOLOGICAL UNCERTAINTIES THEREIN

parameter	max.deviation
Si_3N_4 thickness	1% (1.5 nm)
Si_3N_4 index	$5 * 10^{-4}$
cladding SiO_2 index	$2 * 10^{-3}$
substrate SiO_2 index	$1 * 10^{-4}$
h	10% (0.1 nm)
h_2	10% (2 nm)
W	0.2 μm

The design of the converter should aim at minimizing the effect of variations in d on $\Delta N^c_{\mathrm{TE-TM}}$, in that way in the same time minimizing the effects of uncertainties in h and h_2.

The effect of technological uncertainties on the coupling strength cannot be as easily analyzed as their effect on the resonance wavelength, because it requires the (full vectorial) calculation of overlap integrals between adjacent segments. It is clear that the overlap will become strongly dependent on the asymmetry, as was also found by preliminary experiments. In the design study, we will vary h_2 within the range of 5–20 nm. With such h_2 values, it was experimentally found that acceptable coupling lengths of the order 10 mm can be obtained [12].

Now, the influence of the fabrication tolerances on the the resonance wavelength will be worked out more quantitatively. For small variations in the device geometry and in the refractive indexes, the relative shift in the resonance wavelength λ_r can be written as

$$\frac{\Delta\lambda_r}{\lambda_r} = \frac{1}{\Delta N_{\mathrm{TE-TM}}} \sum_{i=1}^{7} \frac{\partial \Delta N_{\mathrm{TE-TM}}}{\partial x_i} \Delta x_i \qquad (6)$$

where higher-order (cross) terms are neglected. x_i stands for a layer index or one of the geometrical parameters. In Table I, the maximum deviations in these parameters are given, using the technologies available in our laboratory [16]. If the deviations are relative, as in the case of the geometrical parameters, the absolute deviations for the final structure are given inbetween brackets.

As the materials within the layer system are already chosen, the free parameters in the design are the Si_3N_4 core thickness d, the small etch step h, the deep etch step h_2 and the ridge width W. Above, it was already concluded that the resonance wavelength will be mainly dependent on the core layer thickness d. In Fig. 2, $\partial \Delta N^s_{\mathrm{TE-TM}}/\partial d$ is given as a function of the core thickness for a three- layer slab system. A core thickness of 137 nm results in the required $\partial \Delta N^s_{\mathrm{TE-TM}}/\partial d = 0$.

Using a two-dimensional (2–D) mode solver [17], the influence of variations in the geometrical parameters on $\Delta\lambda_r/\lambda_r$ have been calculated. Using an iterative process for the minimization of $\Delta\lambda_r/\lambda_r$, the optimum system appears to correspond with ($d = 137$ nm, $h = 1$ nm, $W = 4$ μm and $h_2 = 15$ nm). For this system, in Fig. 3, $\Delta\lambda_r/\lambda_r$ is given as a function of these parameters.

In each graph in Fig. 3, the effect of a variation of one of the parameters on $\Delta\lambda_r/\lambda_r$, while keeping the others, constant is shown. Also, the expected maximum deviation in each parameter is indicated. As predicted, the influence of variations in d is orders of magnitude higher than the influence of variations in the other parameters. It can be seen that for both the d and W values, taken in the designed system, $\Delta\lambda_r/\lambda_r$ is at a maximum.

As expected, the influence of h_2 on $\Delta\lambda_r/\lambda_r$ can be neglected with respect to the other terms. This has the consequence that h_2-parameter can be used as a parameter to tune the coupling strength without any effective influence on the resonance wavelength, and hence the grating period required. This implies that, without altering the photolithographic masks, converters with

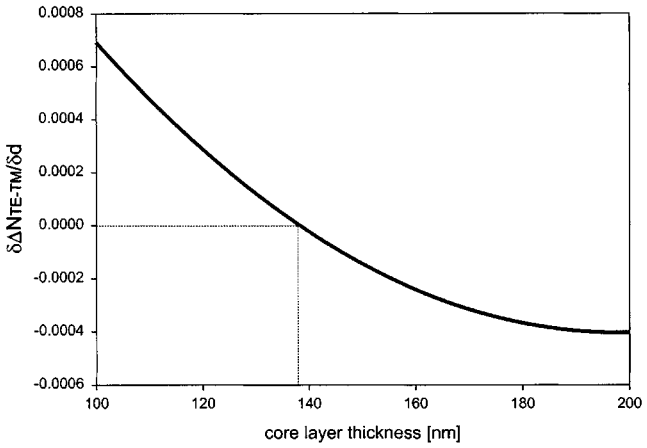

Fig. 2. $\partial \Delta N^s_{\mathrm{TE-TM}}/\partial d$ versus the core layer thickness.

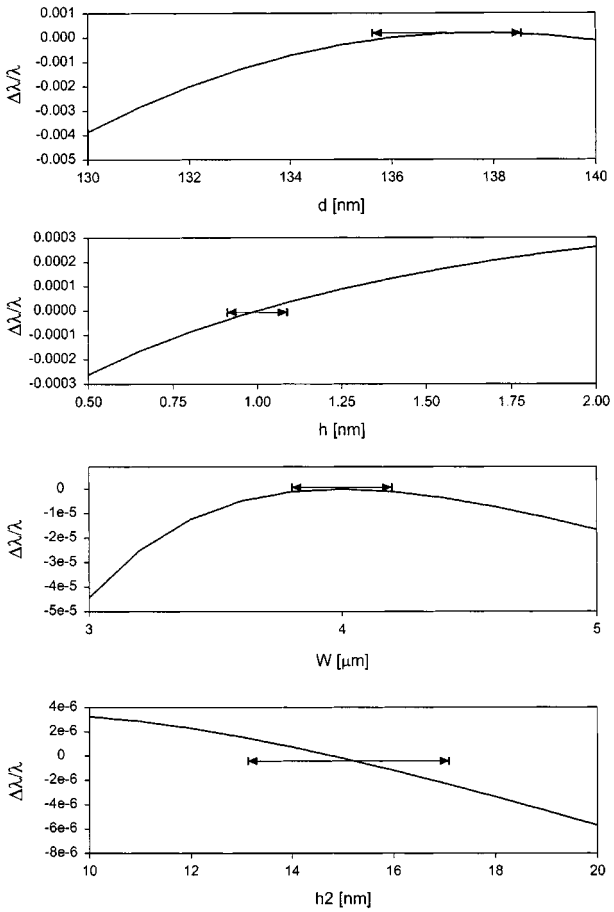

Fig. 3. The effect of technological deviations on $\Delta\lambda_r/\lambda_r$.

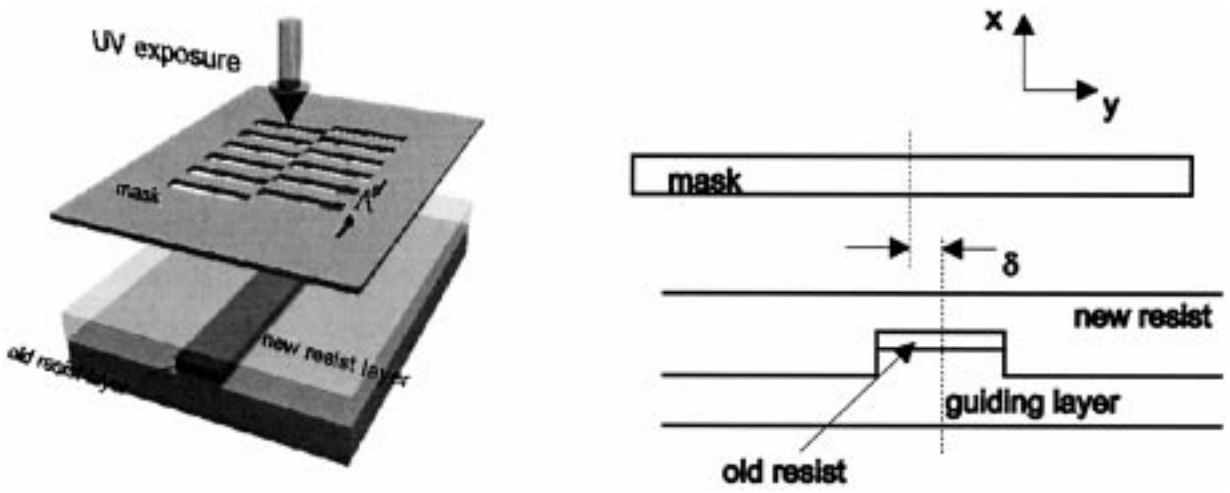

Fig. 4. The double-etch step technique for lowering the tolerances regarding the alignment of the grating mask to the waveguide mask.

different amounts of polarization conversion can be obtained by varying the etching time for defining h_2 only.

Up to now, only the effect of deviations in the geometrical parameters of the layers have been taken into account. For the aforementioned waveguide system, the effects of deviations of the refractive indexes on $\partial(\Delta\lambda_r/\lambda_r)/\partial n$ can be calculated to be -0.2 for the SiO_2 cladding layer, 0.32 for the Si_3N_4 core layer and -0.2 for the SiO_2 substrate layer.

Now, the maximum deviation (worst case analysis) in the resonance wavelength due to technological fluctuations can be calculated to be

$$\Delta\lambda_r = 655 * 0.0038 = 3.8\,\text{nm} \tag{7}$$

where the largest contribution to this deviation arises from variations in the cladding SiO_2 refractive index.

The full width half maximum (FWHM) bandwidth of a codirectional grating assisted coupler with a length of 10 mm is approximately 15 times smaller than 3.8 nm. This implies that for proper performance, a system with a strongly increased coupling strength, and thereby an increased FWHM, or adjustment by tuning the resonant wavelength or adjustment of the wavelength entering the converter is necessary. This is addressed also in Section IV Section IV of this paper.

III. Fabrication

The devices are fabricated on 3" silicon wafers. The substrate SiO_2 layer is grown by thermal oxidation of the silicon wafer, the core layer deposited using low-pressure chemical vapor deposition (LPCVD) and the cladding layer deposited using plasma-enhanced chemical vapor deposition (PECVD) applying the processes as developed in our laboratory [16]. The 1-nm-high ridge was defined using BHF etching (0.55 nm/min), the 15-nm-deep etch step by reactive ion etching (RIE).

In order to increase the fabrication tolerance with respect to mask alignment, a double-masking technique [18] was used to define the deep etch step, see Fig. 4. After definition of the waveguide structure, the positive resist was given a heat treatment in order to make it insensitive to UV exposure, after which a second resist layer was spin coated on top of the old layer. Then, using a mask as shown in Fig. 4, the structure for the deep-etch step was defined in the second resist layer. Using this double masking technique, there is an alignment tolerance equal to the width of the waveguide, here being $2\,\mu$m. Also, it is guaranteed that the etch step is only at the sides of the ridge. In Fig. 5, a micrograph of the converter structure after development of the second photo resist layer is shown.

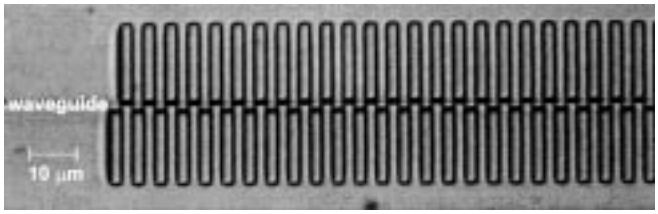

Fig. 5. Micrograph of the waveguide and grating structure in the photoresist layers.

IV. Experimental Results

The converters have been characterized using an argon-pumped (515-nm) dye laser (DCM dye, 620–680 nm, step size 0.03 nm) as shown in Fig. 6. Different wafers with several converters have been realized in order to investigate the reproducibility of the converter performance on single wafers and from wafer to wafer. The converters have been characterized with respect to the resonance wavelength, their FWHM, the channel and functional losses, and the coupling strength.

In Fig. 7, for a device length of 12 mm and ($h = 1$ nm, $h_2 = 15$ nm, $d = 137$ nm, $W = 4\,\mu$m), the conversion versus the wavelength is shown. It can be seen that the FWHM of the conversion peak is small, 0.25 nm. It can further be seen that the resonance wavelength is not 655 nm, but 657.4 nm. The asymmetry in the side lobs is caused by a position dependent effective index difference along the converter. The on-chip spread in the resonance wavelengths was determined to be smaller than 0.1 nm. By performing measurements at converters on several samples from different batches, it was found that the resonance wavelength was 655.3 nm with deviations smaller than 4.3 nm,

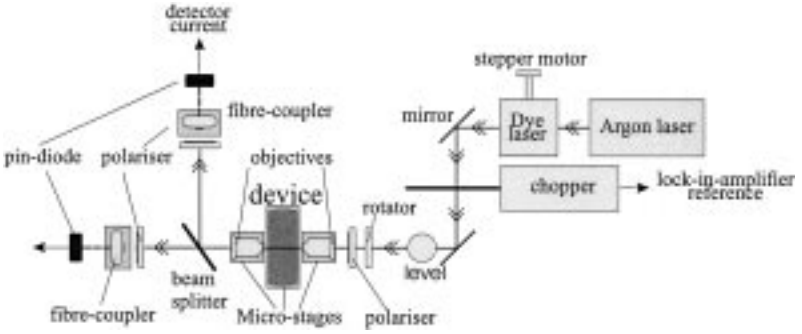

Fig. 6. The experimental setup.

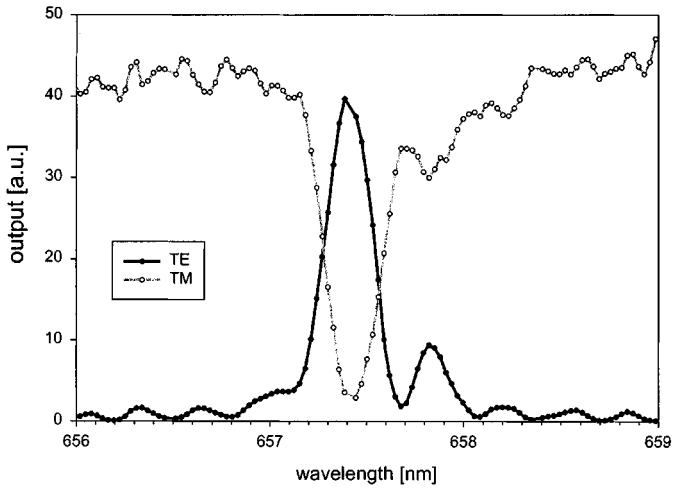

Fig. 7. Typical measured wavelength response of the polarization converter.

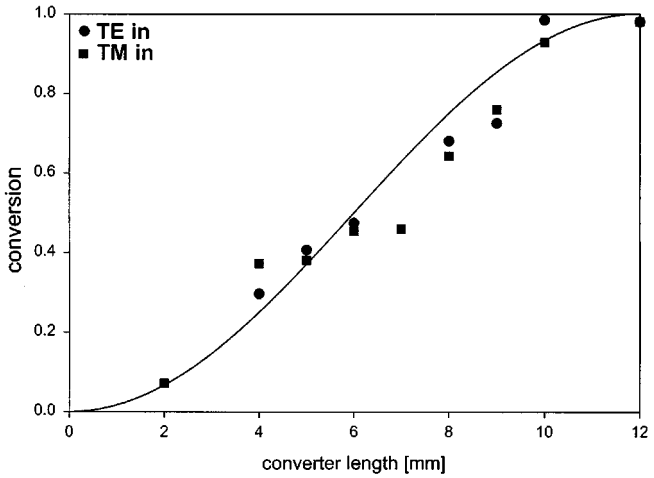

Fig. 8. Device length versus the polarization conversion PC.

i.e., a maximum shift $\Delta\lambda/\lambda = 0.007$, which corresponds well to the predicted value $(655 \pm 3.7\ \text{nm})$ for the resonance wavelength.

Next, loss measurements have been performed regarding the waveguides and the converter. By measuring the scattering on top of the waveguide with a CCD camera and by performing an exponential fit on the intensity versus length dependence, the propagation loss in the waveguide channels was determined to be 1.6 ± 0.1 dB/cm, for both the TE and the TM mode. By measuring the output signals of converters with different length, the functional losses of the converter were determined to be 3 ± 0.3 dB/cm both for TE and TM input light.

Now, with the propagation and functional losses known, the coupling strength of the converters can be determined. For converters on the same wafer having different lengths, the amount of polarization conversion was determined. As for the resonance wavelength the device length and the amount of conversion PC are related by [19]

$$PC = \sin^2(CL) \tag{8}$$

with PC ranging from 0 to 1, where 1 corresponds to a 90° polarization rotation, L is the converter length and C is the coupling strength. In Fig. 8, for converters with ($h = 1$ nm, $h_2 = 15$ nm, $d = 137$ nm, $W = 4\,\mu$m), the polarization conversion (for TE and TM input light) is shown as a function of device length. Complete conversion is obtained at a device length of 12 mm, corresponding to a coupling strength of $6.5 \times 10^{-5}\ \mu\text{m}^{-1}$. This corresponds to a very small rotation of the polarization axis of 0.011° at each transition. Devices with an etch step of 8 nm showed complete conversion for a length of 16 mm, corresponding to a coupling strength of $4.9 \times 10^{-5}\ \mu\text{m}^{-1}$.

Devices with deeper etch steps have been realized in order to obtain converters with higher coupling strengths. However, it was found that for these devices the losses increased rapidly when increasing the depth of the etch step. Experimentally, it could not be discerned whether this was due to an increased scattering as a result of an increase in the surface roughness or as a result of an increased mode mismatch, e.g., increased coupling losses between adjacent segments. However, from BPM simulations no significant increase in the losses at higher h_2 values were found, so, most likely, the experimentally found loss increase has to be ascribed to an increase of the effects of the surface roughness.

The maximum amount of polarization conversion that was measured was 98% for both TE and TM light launched into the converter. Taking the FWHM of the converter response and the line width of the dye laser into account, this is the maximum conversion that can be obtained with our experimental setup. Therefore, as for several samples a conversion of 98% was measured, the conversion might even be higher for light with a smaller linewidth.

For the resonance wavelength, 655 ± 4.3 nm was found, while the FWHM was 0.25 nm. Therefore, it is not assured that for each converter, the desired amount of conversion is achieved

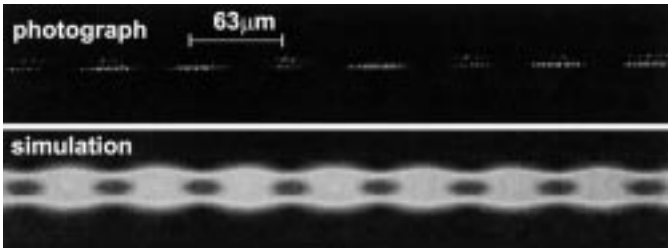

Fig. 9. Micrograph of the beat pattern (top) and BPM simulation of the same structure (same scale).

TABLE II
COMPARISON OF THE CONVERTER PRESENTED HERE WITH CONVERTERS KNOWN FROM LITERATURE

	this paper	**Lang** [11]	**tol** [22]	**merthens** [8]
principle	grating	grating	grating	hybrid modes
material	SiO_xN_y	ion exchanged glass	InP	InP
technology	+	+	–	++
max. conv.	98%	99%	93%	93%
coupling length	12 mm	18mm	1 mm	0.25mm
losses	3 dB	0.4dB	10dB	?
ΔW_{FWHM}	0.25nm	"large"	$\approx$ 30 nm	?
$\Delta\lambda/\lambda_{res}$	0.007	?	?	?

for the desired operation wavelength. Several solutions to this problem can be considered. The first is to make the coupling strength C stronger, resulting in a widening of the FWHM approximately inversely proportional to C. However, in order to increase C, the asymmetry has to be increased, which was experimentally shown to have the drawback of a strong increase of the functional losses. A second solution would be the use of a broad-band lightsource centered around λ_r having a spectral output wider than 8.6 nm, combined with a filter that can be tuned to the resonance wavelength of the polarization converter, or, even better, to the wavelength where the conversion shows its intended value. Alternatively, a tunable lightsource could be applied. The third option, which is currently being investigated, is thermally tuning the resonance wavelength of the converter itself. Preliminary calculations show that within a temperature range of approximately 70° C of the heater electrode, a tuning range of 10 nm can be covered. A more quantitative analysis of the thermally tuned polarization converter will be given elsewhere [7].

When launching TM polarized light into the converter and looking on top of the structure with a microscope, a beat pattern with a period of 63 ± 5 μm could be observed, see Fig. 9. This beat pattern corresponds to an effective index difference of 0.01 between the two beating modes. This beating was present not only for the resonance wavelength, but also for other wavelengths ranging from 620 to 680 nm, with a variation in the beat period of about 3 μm, so it is not specifically related to the polarization conversion process. A 2-D BPM simulation, using the EIM, of the converter structure showed a similar beat pattern with much the same period of 67 ± 2 μm over a wavelength range 620–680 nm. For TE polarized light similar results were obtained. The simulation showed a fringe visibility of 0.08 between the modes, indicating a weak coupling of the zeroth-order (TM) mode to another mode. As the beating is not only present for the resonance wavelength of the converter, the beating must be between two different TM modes. The question arises as to which other mode is involved in the beat pattern.

The effective index difference between both modes is 0.01, so as the N_{eff} of the TM_{00} mode is 1.60, the effective index of the other mode must be 1.59. As the channel structure is mono modal, the second mode cannot be another channel mode. Therefore, the beat pattern must be between the lowest order TM mode and a leaky (radiation) mode in the lateral direction. Because the effective index of the zeroth-order mode in a slab waveguide with a thickness of 136 nm (i.e., the slab region defined by the d–h ridge step) is 1.5995 and in a slab waveguide with a thickness of 122 nm (i.e., the slab region defined by the d–h_2 deep etch step) 1.5775, the unknown radiation mode may be a radiation mode launched into the 136-nm-thick slabguide fragments, its propagation direction deviating approximately 6° from the channel axis. The BPM simulations also show that the propagation losses increase rapidly with increasing grating period, which supports the idea of the existence of a radiation mode: for larger grating periods the radiation, generated at a certain transition is more distanced from the channel axis at the next transition, so at this transition the modal overlap with the guided mode decreases and less power is coupled back to the guided mode. Another indication pointing toward coupling with radiation modes is the following: calculations using a full vectorial mode solver [20] showed that the absolute square of the field-overlap integral of TM modes in adjacent grating segments is low, namely 0.6 only. Therefore, if the radiation modes should not couple back to the guided mode, the functional losses would be 7×10^4 dB/cm. Since the functional losses while propagating through a structure with 1500 periods are 3 dB only, most of the energy transferred to the radiation modes must be coupled back to the guided channel mode. One can wonder whether this radiation mode might be involved in the polarization conversion process in the same way as the higher-order TE_{10} mode was in the systems, reported in [21]. However, because both the wavelength and device length dependence of the conversion correspond completely to the model of a simple codirectional grating assisted coupling between two guided modes, we expect only the zeroth-order TE and TM mode to be involved in the conversion process.

V. DISCUSSION

In Table II, the converter presented here is compared with other passive converters known from literature.

From this table, the following observations can be made:

- The converter presented in [11] showed a slightly higher conversion for a longer length (18 mm), and the functional losses are lower due to graded index profiles obtained by using ion exchange technology instead of etching techniques. Similar to our converter, the realization of this structure is also simple.
- Compared to the structure in [22], our structure shows a higher conversion, lower losses and is technologically simpler. However, the structure in [22] is much shorter $(< 1 \text{ mm})$ as, due to the high refractive index contrast, the coupling can be made much stronger, also resulting into a much larger FWHM value.

- The converter presented in [8] showed a conversion of 93% for the very short length of 0.25 mm (converter losses were not mentioned) and could be realized in a single step. However, for this type of converter, a strongly hybrid character of the propagating modes is required. Also, for filtering applications this converter is not suited as the wavelength dependence is low.

The type of converter best suited for a specific application depends strongly on the required complexity of the optical circuitry and the tolerance with respect to optical losses. If the converters have to be implemented in a complicated optical circuit and high losses and costs are tolerable, InP devices are favored, as due to the high-index contrast not only small converters are obtained, but also small bending radii are feasible, thereby allowing for a large optical functionality per square mm. If the converters have to be implemented in simple low-functionality circuits where large bending radii are tolerable and if low losses are required, the converters fabricated in ion exchanged glass technology are most promising. The SiON type converter presented here is most suited for moderately complicated circuits with moderate demands regarding losses, i.e., the "middle-of-the-road" type of device, as SiON technology combines the possibility of relatively small bending radii with moderately low losses.

Our passive converter is based on a geometrically induced asymmetrical perturbation of the waveguide cross sections. For the realization of these perturbations, no specific crystal structure is required, so this type of converter can be implemented into every material system. Tailoring the design to the technological tolerances results into small maximum deviations of the resonance wavelength from its design value, allowing for matching both values by thermooptical tuning. The small FWHM of the conversion versus wavelength makes it an interesting option as a wavelength selective component in filtering applications, especially in combination with the thermal tuning ability of a slightly modified device; the tuning range being about 10 nm [7].

Passive polarization converters can be applied in either integrated optical sensors or in telecommunication circuits. Currently, in our laboratory the converter has been successfully implemented in several integrated optical sensing platforms, such as a fully integrated optical polarimeter [14] and a differential absorption sensor [23]. In these circuits, the converters are used for partial conversion of a launched TE mode into a TM-polarized mode and also for obtaining the interference of TE- and TM-polarized zeroth order modes. In both sensing systems, the converter acts like wavelength specific $\lambda/4$ wave plates.

Due to the wavelength dependence of the conversion, in principle, the polarization converter can also be used as a wavelength selective component in telecommunication circuits. Using our polarization converter with a thermooptical tuning facility [7], the add–drop multiplexer (ADM) described in [3] can be realized in a technologically simpler and cheaper way. The specific application of these ADMs depends on the width of the conversion response, which is related to the device length. In our converter, with a coupling length of 12 mm, around 1550 nm minimum channel separations of 2 to 3 nm are feasible, excluding its applicability in ADMs for dense wavelength multiplexing. However, it is useful in applications in which the channel spacing is wider, for example, in local area networks (LAN) [24], where channel spacings up to 10 nm are used. Also in high speed systems where the channel spacing is relatively wide, an ADM based on the presented converter should be an option, provided that a flat band response can be obtained for the add and drop channel [25]. This is expected to be feasible by introducing apodization and a phase shift in the grating [26].

VI. Summary

A passive asymmetrical grating-based $\mathrm{TE}_{00} \leftrightarrow \mathrm{TM}_{00}$ –polarization converter in SiON technology has been developed. An analysis of the system is given, in which much attention has been paid to minimizing the effects of technological uncertainties in the fabrication process, which may degrade the system performance. Based on this analysis, the physical layout of the converter has been defined. By using a double-masking technique, the fabrication of the device is very tolerant with respect to the alignment of the grating mask to the waveguide mask. Several converters have been realized, on different wafers and in different batches. The experimentally determined resonance wavelength was 655.3 ± 4.3 nm, matching well the theoretically predicted value of 655 ± 3.7 nm. The on-chip variation in the resonance wavelength was smaller than 0.1 nm. The device losses of the converter are 3 ± 0.3 dB/cm for both TE and TM polarization. Ninety-eight percent conversion has been obtained for a converter with a length of 12 mm. An experimentally observed beat pattern in the converter could be explained (using 2-D BPM simulations) as being due to a leaky mode, which is captured in the grating structure. The converter has already been successfully applied in two types of sensors. Also, due to the narrow wavelength response, the converter offers the potential of implementation as a wavelength selective element in ADM's.

Acknowledgment

The authors thank N. Posthuma for his technological assistance.

References

[1] K. Okamoto, K. Takiguchi, and Y. Ohmori, "16-channel optical add/drop multiplexer using silica-based arrayed-waveguide gratings," *Electron. Lett.*, vol. 31, pp. 723–724, 1995.

[2] C. Stamm and W. Lukosz, "Integrated optical difference interferometer as immunosensor," *Sensors and Actuators B*, vol. 31, pp. 203–207, 1996.

[3] F. Wehrmann, C. Harizi, H. Herrmann, U. Rust, W. Sohler, and S. Westenhofer, "Integrated optical, wavelength selective acoustically tunable 2×2 switches (add-drop multiplexers) in $linbo_3$," *IEEE J. Select. Topics Quantum Electron.*, vol. 2, pp. 263–296, 1996.

[4] Y. Shani, R. Alferness, T. Koch, U. Koren, M. Oron, B. I. Miller, and M. G. Young, "Polarization rotation in asymmetric periodic loaded rib waveguides," *Appl. Phys. Lett.*, vol. 11, pp. 1278–1280, 1991.

[5] F. Heismann, L. L. Buhl, and R. C. Alferness, "Electro-optically tunable, narrowband $Ti : linbo_3$ wavelength filter," *Electron. Lett.*, vol. 23, pp. 572–574, 1987.

[6] Z. Tang, O. Eknoyan, H. F. Taylor, and V. P. Swenson, "Tunable guided-wave optical polarization converter in lithium tantalate," *Appl. Phys. Lett.*, pp. 1059–1061, 1993.

[7] T. M. Koster and P. V. Lambeck, "Thermally tunable polarization converter," , submitted for publication.

[8] K. Mertens, B. Opitz, R. Hovel, K. Heime, and H. J. Schmitt, "First realized polarization converter based on hybrid supermodes," *IEEE Photon. Technol. Lett.*, vol. 10, pp. 388–390, 1998.
[9] V. P. Tzolov and M. Fontaine, "A passive polarization converter free of longitudinally-periodic structure," *Opt. Commun.*, vol. 127, pp. 7–13, 1996.
[10] J. J. G. M. van der Tol, F. Hakinzadeh, J. W. Pedersen, H. van Brug, and D. li, "A new short and low-loss passive polarization converter on InP," *IEEE Photon. Technol. Lett.*, vol. 7, pp. 32–34, 1995.
[11] T. Lang, F. Bahnmuller, and P. Benech, "New passive polarization converter on glass substrate," *IEEE Photon. Technol. Lett.*, vol. 10, pp. 1295–1297, 1998.
[12] T. M. Koster and P. V. Lambeck, "Fabrication tolerant passive polarization converter realized in SiON technology," in *Proc. LEOS Benelux Chapter*, Gent, Belgium, Nov. 26, 1998, pp. 117–120.
[13] C. M. Weinert and H. Heidrich, "Vectorial simulation of passive te/tm mode converter devices on inp," *IEEE Photon. Technol. Lett.*, pp. 324–326, 1993.
[14] T. M. Koster, N. E. Posthuma, and P. V. Lambeck, "Fully integrated optical polarimeter," in *Proc. Euro. (r)ode V*, Lyon, France, April 16–19, 2000.
[15] H. Kogelnik and V. Ramaswamy, "Scaling rules for thin-film optical waveguides," *Appl. Opt.*, vol. 13, pp. 1857–1862, 1974.
[16] K. Worhoff, A. Driessen, P. V. Lambeck, L. T. H. Hilderink, P. W. C. Linders, and T. J. A. Popma, "Plasma enhanced chemical vapor deposition silicon oxynitride optimized for application in integrated optics," *Sensors Actuat. A*, vol. 74, pp. 9–12, 1999.
[17] *2d mode solver selene*. Enschede, The Netherlands: bbv software bv.
[18] E. C. M. Pennings, "Bends in optical ridge waveguides : modeling and experiments," Ph.D. dissertation, Univ. Delft, Delft, The Netherlands, 1990.
[19] H. Berends, "Integrated optical bragg reflectors as narrowband wavelength filters," Ph.D. dissertation, Univ. Twente, Enschede, The Netherlands, 1997.
[20] *Fimmwave, 2d Vectorial Mode Solver, Photon Design.* Oxford, U. K..
[21] K. Mertens, B. Scholl, and H. J. Schmitt, "Strong polarization conversion in periodically loaded strip waveguides," *IEEE Photon. Technol. Lett.*, vol. 8, pp. 1133–1135, 1998.
[22] J. J. G. M. van der Tol, J. W. Pedersen, E. G. Metaal, Y. S. Oei, F. H. Groen, and I. Moerman, "Efficient short polarization converter," in *Proc. ECIO 1995*, Delft, The Netherlands, 1995, pp. 319–322.
[23] T. M. Koster and P. V. Lambeck, "Integrated optical platform for absorptive sensing of chemical concentrations using chemo-optical monolayers," Sensors and Actuat. B, submitted for publication.
[24] B. E. Lemoff, L. B. Aronson, and L. A. Buckman, "A low cost multi wavelength local area network," *Hewlett Packard J.*, pp. 42–52, 1997.
[25] C. K. Madsen and J. H. Zhao, *Optical Filter Design and Analysis: A Signal Processing Approach.* New York: Wiley, 1999.
[26] B. E. Little, C. Wu, and W. P. Huang, "Synthesis of ideal window filter response in grating-assisted couplers," *Opt. Lett.*, vol. 21, pp. 725–727, 1996.

Ton Koster was born in the Netherlands in 1970. He received the M.Sc. degree in physics and the Ph.D. degree from the University of Twente, Enschede, The Netherlands, in 1995 and 2000, respectively.

Since 2000, he has been with IBM-Zurich, Zurich, Switzerland, where he focuses on the design of integrated optical devices for optical telecommunications.

Paul V. Lambeck received the M.Sc. degree in physical chemistry from the University of Amsterdam, Amsterdam, The Netherlands, and the Ph.D. degree from the University of Twente, Enschede, The Netherlands.

He joined the faculty of the University of Twente in 1964, and is currently an Associate Professor and Group Leader of the Integrated-Optics Group of the MESA+ Institute of the University of Twente. His research interests include optical sensors, mechanooptical devices, and integrated optical amplifiers and switches.

Dr. Lambeck is a member of the Optical Society of America.